

Published in final edited form as:

Biomaterials. 2012 February ; 33(5): 1607–1617. doi:10.1016/j.biomaterials.2011.11.011.

Skin permeating nanogel for the cutaneous co-delivery of two anti-inflammatory drugs

Punit Shah, Pinaki Desai, Apurva Patel, and Mandip Singh*

College of Pharmacy and Pharmaceutical Sciences, Florida A&M University, Tallahassee, FL 32307, USA

Abstract

The aim of this study was to develop an effective drug delivery system for the simultaneous topical delivery of two anti-inflammatory drugs, spantide II (SP) and ketoprofen (KP). To achieve this primary goal we have developed a skin permeating nanogel system (SPN) containing surface modified polymeric bilayered nanoparticles along with a gelling agent. Poly-(lactide-co-glycolic acid) and chitosan were used to prepare bilayered nanoparticles (NPS) and the surface was modified with oleic acid (NPSO). Hydroxypropyl methyl cellulose (HPMC) and Carbopol with the desired viscosity were utilized to prepare the nanogels. The nanogel system was further investigated for *in vitro* skin permeation, drug release and stability studies. Allergic contact dermatitis (ACD) and psoriatic plaque like model were used to assess the effectiveness of SPN. Dispersion of NPSO in HPMC (SPN) produced a stable and uniform dispersion. *In vitro* permeation studies revealed increase in deposition of SP for the SP-SPN or SP+KP-SPN in the epidermis and dermis by 8.5 and 9.5 folds, respectively than SP-gel. Further, the deposition of KP for KP-SPN or SP+KP-SPN in epidermis and dermis was 9.75 and 11.55 folds higher, respectively than KP-gel. Similarly the amount of KP permeated for KP-SPN or SP+KP-SPN was increased by 9.92 folds than KP-gel. The ear thickness in ACD model and the expression of IL-17 and IL-23; PASI score and TEWL values in psoriatic plaque like model were significantly less ($p < 0.001$) for SPN compared to control gel. Our results suggest that SP+KP-SPN have significant potential for the percutaneous delivery of SP and KP to the deeper skin layers for treatment of various skin inflammatory disorders.

1. Introduction

In the last decade, an increasing number of investigations concerning the use of nanoscale structures for drug and gene delivery purpose have been reported. Nanocarriers have been investigated for delivery of drugs to the specific anatomical sites such as brain [1], eyes [2], lungs [3], intestine [4], nose [5] and skin [6] etc. To improve the notoriously low drug absorption from the skin surface, nanoparticulate carriers have proven to be efficient and advantageous. Development of successful topical/transdermal drug delivery systems has been limited in scope due to the significant penetration barrier provided by the stratum corneum (SC) whose composition limits the application of number of suitable drugs for topical and transdermal delivery. However, there is a growing interest in the development of

© 2011 Elsevier Ltd. All rights reserved.

*Corresponding Author: Mandip Singh, College of Pharmacy and Pharmaceutical Sciences, Florida A & M University, Tallahassee, FL 32307. Tel: (850) 561-2790; Fax: (850) 599-3347. mandip.sachdeva@gmail.com.

Publisher's Disclaimer: This is a PDF file of an unedited manuscript that has been accepted for publication. As a service to our customers we are providing this early version of the manuscript. The manuscript will undergo copyediting, typesetting, and review of the resulting proof before it is published in its final citable form. Please note that during the production process errors may be discovered which could affect the content, and all legal disclaimers that apply to the journal pertain.

efficient targeted drug delivery systems to physiological sites in the skin [7]. Several attempts have been made and are still under investigation to develop topical formulation of macromolecules for the treatment of various skin diseases. Currently, these diseases are principally treated with topical corticosteroids that target a variety of pathways of the inflammation cascade [8]. However, clinical use of corticosteroid therapy is limited due to associated local side effects such as skin atrophy, telangiectasia, acne and secondary infections as well as contact dermatitis and perioral dermatitis. Spantide II (SP), a neurokinin1 (NK1) receptor antagonist, is a neuropeptide with known anti-inflammatory activity [9–10]. Combination of a **new** neuropeptide, SP, along with ketoprofen (KP), a well known potent non-steroidal anti-inflammatory drug (NSAID) [11] in a topical formulation will have great impact for the treatment of skin disorders with minimal adverse effects.

In the field of dermatology and cosmetology, micro and nano sized particles have been thoroughly investigated and some formulations are already commercially available. Recently solid lipid nanoparticles (SLN), nanostructured lipid carriers (NLC) and lipid nanocapsules have shown improved drug permeation through the skin. However due to their limited drug loading and phase stability issue, their application for clinical use is restricted. Therefore, increased attention has been given to polymeric nanoparticles. Various **non-toxic** and biodegradable synthetic or semi-synthetic polymers, including polylactic acid (PLA) [12], poly(lactic-*co*-glycolic acid (PLGA) [13], poly(ϵ -caprolactone) [14], chitosan [15] have shown promising results for topical drug delivery. These polymeric nanoparticles offer advantages of controlled and sustained release via modification of polymer composition and reducing irritation associated with direct contact of drug with skin.

PLGA based nanoparticles have been extensively studied since they offer number of advantages for skin delivery including **non-toxicity and** biodegradability, by hydrolysis leading to formation of water and carbon dioxide and entrapment of various therapeutic moieties [16]. Drug delivery into the skin by PLGA nanoparticles can be enhanced by modifying the particle surface with a cationic polymer such as chitosan. Chitosan is a cationic polysaccharide with many interesting biopharmaceutical properties, such as **non-toxicity**, biodegradability, bioadhesion and has been extensively used as a penetration enhancer in topical formulations [17]. The surface modification of the PLGA nanoparticles with chitosan can be advantageous for topical delivery in many aspects, such as (a) ability to incorporate two drugs in inner and outer layers of the nanoparticles, (b) increased stability of the macromolecules like SP which can be encapsulated in the PLGA inner core, (c) reversal of zeta potential promoting skin adhesion and thus enhancing skin delivery and (d) ability to conjugate with other molecules such as penetration enhancer through the free amino groups of chitosan. When polymeric nanoparticles were used for topical drug delivery, it was observed that the drug permeation was enhanced by gradual drug release from the nanoparticles on the skin surface but the intact nanoparticles were unable to permeate in deeper skin layers [18–19]. Other attempts to verify the penetration of nanoparticles across the skin were met with little success, where only few of the researchers were able to show permeation of nanoparticles into the skin passively through the hair follicles while most of the nanoparticles were primarily restricted to the uppermost layers of the SC and unable to permeate the skin.

The most extensively investigated enhancement strategy for the skin delivery involves the use of chemicals that can reversibly compromise the skin's barrier function and consequently allow the entry of poorly penetrating molecules into the skin. One of the widely investigated penetration enhancers is oleic acid (OA), a monostructured fatty acid and a membrane fluidizing agent. OA is a FDA approved potent chemical permeation enhancer and is widely used in commercial formulations. OA extracts a fraction of the endogenous SC membrane compounds, promoting phase separation in the SC membrane

system. Reducing the proportion of crystalline lipids and creating more permeable OA-rich domains can lead to enhancement effect of the drugs into the skin [20]. Electron microscopic studies have suggested that lipid domain is stimulated within the SC bilayer lipids upon exposure to OA [21]. The formation of such pools provides permeability defects within the lipid bilayers and thus facilitates the permeation of macromolecules into the deeper epidermal and dermal layers. Therefore, surface modification of PLGA-chitosan bilayered nanoparticles with OA (NPSO) can open the channels in the SC, which can enhance the delivery of incorporated active drugs into deeper skin layers where the site of action is present for the inflammatory skin diseases.

One of the limitations of topical dosage forms is the relatively short lasting time of the active drugs at the application site. In order to obtain prolonged skin retention and controlled release for the desired therapeutic effect, it is appropriate to incorporate NPSO into a proper gel matrix (Nanogel system). Hydrophilic polymers are considered most suitable for topical applications, but type and concentration of the polymer forming gel matrix can influence the stability and release rate of the drugs [22]. Nanogels are nano-sized network of chemically or physically cross linked polymer particles. The gel can aid in creating a uniform dispersion of the nano-carriers in the matrix and increases the contact time which results in enhanced skin penetration of the drug payload [23]. In the present study, we hypothesize that incorporating the surface modified bilayered PLGA-Chitosan nanoparticles with OA into a skin penetrating nanogel system (SPN) can further increase the efficiency by maximizing skin contact time and preventing the 'run-off' effect associated with aqueous nanoparticle dispersion.

The specific aims of this research were to: (1) prepare SPN for SP and KP loaded bilayered nanoparticles, where SP was loaded into PLGA inner core and KP was incorporated into the chitosan outer layer; (2) formulate SPN using hydroxypropyl methyl cellulose (HPMC) or Carbopol and characterize for rheological behavior to get optimum viscosity without affecting particle size of nanoparticles; (3) study the effect of NPSO and SPN for *in vitro* human skin permeation and (4) compare the therapeutic efficacy of the SPN in an *in vivo* allergic contact dermatitis (ACD) and a psoriatic plaque like model with a marketed formulation of tacrolimus, Topgraf[®] (GlaxoSmithKline Pharmaceuticals Limited, Thane, India).

2. Materials and Methods

Poly(lactic-co-glycolic acid) (PLGA) was purchased from PURAC biomaterials (Lincolnshire, IL). Polyvinyl alcohol (PVA), chitosan, dichloromethane, tween 80, sodium tripolyphosphate (TPP), polyethylene glycol 400 (PEG-400), phosphate buffer saline sachets (PBS, pH 7.4), trifluoroacetic acid (TFA) and 2,4-dinitrofluorobenzene (DNFB) were purchased from Sigma-Aldrich Co (St Louis, MO). HPLC grade of acetonitrile, water and ethanol were purchased from Sigma-Aldrich Co (St Louis, MO). Oleic acid-PEG-succinimidyl glutarate ester (OA) was custom synthesized from Nanocs Inc (New York, NY). Ketoprofen (KP) was purchased from Spectrum chemical mfg corp. (Gardena, CA). Spantide II (SP) was purchased from American peptide company Inc, (Sunnyvale, CA). Hydroxy propyl methyl cellulose (HPMC; METHOCEL[™] K4M Premium CR Grade) was generously gifted by DOW Chemical Company (Midland, MI). Carbopol (Carbopol 981[®] NF) was generously gifted by Lubrizol Advanced Materials, Inc. (Cleveland, OH). Imiquimod (IMQ) was purchased from VWR International (Suwanee, GA). Topgraf[®] (tacrolimus ointment 0.1%) was purchased from GlaxoSmithKline Pharmaceuticals Limited (Thane, India). IL-17 and IL-23 antibodies along with ABC staining immunohistochemistry kit were purchased from Santa Cruz Biotechnology Inc (Santa Cruz, CA).

2.1 Preparation of Surface modified bilayered nanoparticles (NPSO)

Bilayered nanoparticles (NPS) were prepared by modified emulsion solvent evaporation method [24]. Briefly, 10 mg of PLGA was dissolved in 1.5 ml of dichloromethane. The organic phase was added to 20 ml of 0.1% w/v PVA solution comprising 4 ml of 0.5% w/v chitosan and 1.5 ml of tween 80 with constant stirring to form a coarse emulsion. This emulsion was broken down into nanodroplets by high speed homogenization for 15 min at 30,000 rpm. The nanoparticles were stirred for 30 min to evaporate the organic phase. Five milliliters of the nanoparticles dispersion was transferred to a scintillation vial. The chitosan, present on the outer layer of nanoparticles was then cross linked with 100 μ l of 1% w/v TPP to prepare NPS. This prepared NPS dispersion was stirred at 300 rpm for 2 h to ensure complete cross-linking of chitosan.

The SP nanoparticles (SP-NPS) were prepared by dissolving spantide II and phosphatidylinositol (PI) in ethanol and then mixed with organic phase containing PLGA. NPS were prepared by homogenization as described above. To this nanoparticulate dispersion, TPP was added for cross-linking of chitosan coat. To prepare SP and KP nanoparticles (SP+KP-NPS), ketoprofen was dispersed in the 1% w/v TPP and added drop wise to SP-NPS. To prepare KP nanoparticles (KP-NPS), SP was excluded from the NPS preparation technique.

For surface modification, NPS was suspended in phosphate buffer, pH 8.0 and incubated for 2 h with OA (mole ratio of chitosan to OA in 1:6), previously dissolved in 10 μ l of DMSO. The surface modified NPS were represented as KP-NPSO, SP-NPSO and SP+KP-NPSO for ketoprofen, spantide II, and a combination of spantide II and ketoprofen, respectively.

NPS and NPSO were characterized for particle size and zeta potential using Nicomp 380 ZLS (Particle Sizing Systems, Port Richey, FL). Further the drug content and entrapment efficiency was characterized as reported by Patlolla et al [25]. TNBS method was performed to estimate the percent of surface accessible amino groups by colorimetric reaction [26].

2.2 Preparation of a skin permeating nanogel (SPN)

The topical formulation for delivery to the skin should have adequate rheology. Therefore SPN of desired viscosity was prepared by incorporating various thickening agents in the NPSO dispersion. HPMC or Carbopol was added to NPSO aqueous dispersion with constant stirring until complete gel formation. Thereafter, the SPNs were allowed to stabilize at room temperature for 24 h. For Carbopol, the SPNs were neutralized by drop-wise addition of triethanolamine (pH = 7.0) and were further stabilized at room temperature for 24 h before use. The nanogel comprising SP+KP-NPSO, SP-NPSO and KP-NPSO were represented as SP+KP-SPN, SP-SPN and KP-SPN, respectively.

The control gel formulations of SP and KP were prepared by dissolving SP and KP in ethanol and PEG-400 mixture. To this, HPMC was added and mixed slowly at room temperature until a gel formation was complete. This gel containing KP, SP and SP+KP were represented as KP-gel, SP-gel and SP+KP-gel, respectively.

2.3 Rheology of SPNs

The viscoelastic properties of SPNs were investigated using Brookfield Rheocalc® V 32 Rheometer (Brookfield, USA) DV-II model with CP40 spindle using cone and plate geometry. Data analysis was done with Brookfield Rheocalc® 2.010 Application Software. The rheologic properties of the SPN were studied by continuous shear investigations using Brookfield R/SCPS Plus Rheometer (Brookfield, USA), with cone and plate geometry using spindle C25-2 DIN as the measuring system. The shear rate was increased in ascending

order from 0 to 100 D [1/s] (up curve) and then decreased from 100 to 0 D [1/s] (down curve) and the resulting shear stress [D/cm²] was measured. The sample was equilibrated at 28°C prior to each measurement. All measurements were made in triplicate.

2.4 Determination of drug content in SPNs

The SP and KP content in SP+KP-SPN was determined by weighing HPMC gel containing NPSO in a volumetric flask and extracting by shaking it overnight with methanol. Then an aliquot of the extracted sample was filtered through 0.45 µm PTFE filters and drug content was determined by HPLC.

2.5 HPLC analysis

An HPLC system (Waters Corp, Milford, MA) along with a Vydac reverse phase C18 (300 Å pore size silica) analytical column (5µm, 4.6 × 250mm) (GraceVydac, Columbia, MD) were used for the analysis of SP. The mobile phases used for spantide II were 0.1% v/v TFA in water (solvent A) and 0.1% v/v TFA in acetonitrile (solvent B) and they were run at a gradient of 60:40 to 40:60, solvent A:B, respectively for 20 min, with a flow rate of 1.2 ml/min. Spantide II content in the samples was determined at 230 nm.

Waters Symmetry C18 analytical column (5µm, 4.6 × 250 mm) was used for analysis of KP. The mobile phases used was 0.025% v/v TFA in water (solvent A) and acetonitrile (solvent B) and they were run at a gradient of 70:30 for 5 min, then 10:90 for 8 min followed by 0:100, solvent A:B, respectively with a flow rate of 1 ml/min. KP content in the samples was determined at 227.5 nm.

2.6 *In vitro* drug release

The *in vitro* drug release study of SPN was performed to investigate the amount of drug released from a gel. A porous membrane of mol wt cut off 50,000 Da (Sigma-Aldrich Co, MO) was used. The membrane was mounted between the donor and receiver compartments of Franz diffusion cells [27]. The SP-SPN or KP-SPN and SP+KP-SPN were then applied evenly on the surface of the membrane in the donor compartment. The receiver compartment was filled with 0.5% w/v volpo 20 in PBS (pH 7.4), stirred at 300 rpm, and maintained at 37°C ± 0.5°C using a circulating water bath. At predetermined time intervals (1, 2, 4, 6, 8, 12, 22, 24, 48 and 72 h), 0.5 ml samples were collected from the receiver compartment and replaced with fresh buffer solution. The samples collected from receiver compartment were analyzed for drug content using HPLC method.

2.7 Stability studies

The SPNs were filled in the scintillation glass vials and incubated as per ICH guideline at 2–8°C (refrigeration condition) and 40°C/65% RH (accelerated condition) for 3 months. Appearance, clarity were analyzed by visual inspection. The particle size of SPNs was evaluated using Nicomp 380 ZLS (Particle Sizing Systems, Port Richey, FL).

2.8 Human skin permeation studies

Dermatomed human skin was obtained from Allosource (Centennial, CO) with a thickness of 0.5 ± 0.1 mm. Skin was then stored at –80°C until use. The dermatomed human skin was thawed and washed with distilled water for 30 min to remove excess of glycerol. Skin permeation studies were performed using established procedures. The human skin permeation studies were performed by mounting the dermatomed human skin on Franz diffusion cell set up (PermeGear Inc., Riegelsville, PA). The surface area of the dermatomed human skin exposed to the formulation in the donor chamber was 0.64 cm² and the receiver fluid volume was 5 ml. The control gel formulation, NPSO or SPN were applied evenly on

the surface of the human skin in the donor compartment. The skin permeation study was performed using 6 diffusion cells and represented as an average of 6 cells. The receiver compartment was filled with 0.5% w/v volpo 20 in PBS (pH 7.4) and stirred at 300 rpm. The temperature of receiver compartment was maintained at $37^{\circ}\text{C} \pm 0.5^{\circ}\text{C}$ using a circulating water bath to simulate the skin temperature at physiological level. To replicate the clinical conditions, a non-occlusive condition was followed and the surface of the skin was exposed to the surrounding air. After 24 h of skin permeation, the receiver fluid was collected and centrifuged at 13,500 rpm for 15 min and analyzed for drug content using HPLC method.

2.9 Skin extraction

For evaluation of drug retention in dermatomed human skin, the entire dosing area (0.64 cm^2) was collected with a biopsy punch. SC, epidermis and dermis were separated using cryotome. SC, epidermis and dermis were minced and boiled with 250 μl PBS (pH 7.4) separately for 10 min. To these samples 250 μl of acetonitrile was added to solubilize the drug. All the samples were then centrifuged at 13,500 rpm for 20 min. The supernatant was collected and analyzed by HPLC for drug content.

2.10 *In vivo* inflammatory models

2.10.1 Animals—C57BL/6 mice (6 weeks old; Charles River Laboratories, Wilmington, MA) were grouped and housed ($n = 6$ per cage) in cages with Tek-Fresh bedding. The animals were kept under controlled conditions of 12:12 hr light:dark cycle, $22 \pm 2^{\circ}\text{C}$ and $50 \pm 15\%$ RH. The mice were fed (Harlan Teklad) and water ad libitum. The animals were housed at Florida A and M University in accordance with the standards of the Guide for the Care and Use of Laboratory Animals and the Association for Assessment and Accreditation of Laboratory Animal Care (AAALAC). The animals were acclimatized to laboratory conditions for one week prior to experiments. The protocol of animal study was approved by the Institutional Animal Care and Use Committee (IACUC), Florida A&M University, FL.

2.10.2 Allergic contact dermatitis (ACD)—C57BL/6 mice were sensitized on day zero by applying 25 μl of 0.5% v/v DNFB in acetone:olive oil (4:1) on the shaved abdomen. Mice were then challenged on day 5 by epicutaneous application of 25 μl of 0.2% v/v DNFB in acetone:olive oil (4:1) on the right ear in order to induce an ACD response. The left ears were treated with vehicle alone (acetone:olive oil 4:1) and served as an internal control. The ACD response was determined by the degree of ear swelling compared with that of the vehicle treated contra-lateral ear before DNFB challenge. The increase in ear thickness was measured with a vernier caliper (Fraction+ Digital Fractional Caliper, General Tools & Instruments Co., LLC., New York, NY) at 0, 24, 48 and 72 h. Right ears of the mice were treated with topical application of gel or SPNs, 2 h after antigen challenge and 3 times a day thereafter for 3 days. Tacrolimus is a nonsteroidal immunomodulator classified as calcineurin inhibitor. Therefore a marketed tacrolimus formulation, Topgraf[®] was used as a positive control. The ear swelling was measured before application of gel or SPNs. This was considered as 0 h ear thickness. Then the SP+KP gel or SPNs were applied and the ear thickness was measured at 24, 48, and 72 h. The ACD response was determined by taking a difference between 0 h and other time points.

2.10.3 Imiquimod (IMQ) induced Psoriatic plaque like model—This psoriatic plaque like model was developed by modifying the procedure as described by Fits et al. [28]. C57BL/6 mice of age 8–11 weeks were kept under specific pathogen-free conditions. IMQ was used to induce the psoriatic plaque like model. Topical application of its suspension was applied for 5 consecutive days on the shaved back of mice. The dose of IMQ applied (4 mg/day) was optimized based on the induction of skin inflammation. To the

inflamed skin area SP+KP gel or SPN were applied topically every day for 5 days. Topgraf[®] was used as a positive control.

2.10.3.1 Scoring severity of skin inflammation: To score the severity of inflammation on the mice back skin, an objective scoring system was developed based on the clinical Psoriasis Area and Severity Index (PASI) [28]. Erythema, scaling, and thickening was scored independently on a scale from 0 to 4: 0, none; 1, slight; 2, moderate; 3, marked; 4, very marked. The scoring was performed every 24 h for 5 day.

2.10.3.2 Transepidermal water loss (TEWL): Measurement of TEWL was performed for all the treatment and control inflamed skin areas before and after application of SP+KP gel or SPNs as described by Chatterjee et al. [29]. The TEWL was measured every 24 h for 5 days using a TewameterTM210 (Courage Khazaka, Koln, Germany). The probe of the Tewameter TM 210 was placed perpendicular to the surface of the skin and a stable reading of TEWL was noted after 60 sec.

2.10.3.3 Histology: The inflamed skin was collected at the end of experiment and stored in 10 % neutral phosphate buffered formalin. Following fixation, samples were dehydrated and embedded in paraffin. Five- μ m microtome sections of the inflamed skin were then stained with hematoxylin and eosin. The Olympus BX40 light microscope equipped with computer-controlled digital camera (DP71, Olympus Center Valley, PA) was used to visualize the images on the slides.

2.10.3.4 Immunohistochemistry (IHC): IHC study for IL-17 and IL-23 was performed as per the procedure described by Chougule et al. [30]. In brief, formalin-fixed, paraffin-embedded skin sections were used for IHC studies according to the protocol specified in the ImmunoCruz[™] mouse ABC staining kit (SantaCruz Biotechnology Inc, CA). The section slides were washed in xylene and hydrated in different concentrations of alcohol. The slides were incubated with the primary antibody against IL-17 and IL-23 separately overnight at 4°C.

Horseradish peroxidase-conjugated secondary antibody was applied to locate the primary antibody. The specimens were stained with DAB chromogen and counterstained with hematoxylin. The presence of brown staining was considered a positive identification for activated IL-17 and IL-23. The Olympus BX40 light microscope equipped with computer-controlled digital camera (DP71, Olympus Center Valley, PA) was used to visualize the images on the slides.

2.11 Combination Index

Combination Index (CI) value [31] was calculated separately using inflamed ear thickness of ACD model and using TEWL values of psoriatic plaque like model to evaluate the combined effect of SP and KP. The CI was calculated using following equation:

$$\text{Combination Index (CI)} = \frac{\text{Response of Ketoprofen}}{\text{Response of Combination}} + \frac{\text{Response of Spantide II}}{\text{Response of Combination}} \quad \text{Equation 1}$$

1

The CI values were interpreted as follows: CI > 1.3: antagonism, CI = 1.1–1.3: moderate antagonism, CI = 0.9–1.1: additive effect, CI = 0.8–0.9: slight synergism, CI = 0.6–0.8: moderate synergism, CI = 0.4–0.6: synergism, CI = 0.2–0.4: strong synergism.

2.12 Statistical analysis

The SP and KP content of the skin tissue was expressed as mg per g of the tissue. Differences between the skin permeation of SP+KP gel, SP+KP-SPN and Topgraf® were examined using ANOVA and Tukey multiple comparison test. Means were compared between two groups by student's *t* test and between three dose groups by one-way variance analysis (ANOVA). Mean differences with $p < 0.001$ were considered to be significant.

3. Results

3.1 Preparation of surface modified nanoparticles

The mean particle size of SP+KP-NPS was found to be 169 nm with a polydispersity index (PI) of 0.18. After surface modification with OA, the mean particle size of SP+KP-NPSO was increased to 183 nm. The zeta potential of SP+KP-NPSO was decreased from 10.43 to 5.34 mV after surface modification which possibly was because of the reduction in free amine groups of chitosan, available on the surface of nanoparticles. The percent of surface accessible amine groups of SP+KP-NPS were evaluated using TNBS method and were found to be 82 percent after 2 h incubation of SP+KP-NPS with OA. The entrapment efficiency of SP and KP was $92.81 \pm 2.17\%$ and $81.27 \pm 2.26\%$, respectively. The entrapment efficiency of SP and KP was unaffected by surface modification.

3.2 Preparation of gel

For drug release, skin permeation and *in vivo* studies, NPSO was dispersed in the HPMC gel to achieve the final concentration of 0.8% w/v HPMC and then mixed slowly for 2 h in order to form a uniform dispersion. Samples were then allowed to settle at room temperature for 24 h.

3.3 Rheology

The rheological behavior of topical/transdermal formulations was investigated since it relates to the spreadability of the formulation and contact time on the skin surface [32–34]. The effect of different percent of HPMC was evaluated on viscosity profile of SPN formulation (Table 1). The viscosities of SP+KP-SPN comprising 0.4%, 0.8%, 1.2% w/v HPMC were 0.12, 1.16, 13.43 cP, respectively. Particle size of SPN was increased from 183 to 226nm for SPN comprising of 1.2% w/v HPMC. This might be because of the cross-linking of the polymer network. However there was no change in the particles of SPN when prepared using 0.4% w/v and 0.8% w/v HPMC. A plot of the shear rate vs the shear stress of the SPN is shown in Figure 1 demonstrating thixotropic behavior of pseudoplastic system.

3.4 *In vitro* drug release

SP and KP were released in a controlled manner from SPN. SP showed 20% of release within 24 h from NPS (Figure 2a) while KP showed 59% release within 24 h (Figure 2b). Drug release from SP-SPN or SP+KP-SPN was almost similar and followed first order release kinetics with a best fit r^2 value of 0.99. Further KP-SPN or SP+KP-SPN followed Korsmeyer – Peppas release kinetics with a best fit r^2 value of 0.99. Also there was no statistical difference between the drug release from KP-SPN or SP+KP-SPN.

3.5 Stability studies

The mean particles size of SPN was investigated during stability studies as per ICH guidelines. There was no change in the appearance and clarity of SPN found during stability studies. The particle size of SPNs was unchanged when stored at refrigeration temperature. However the particle size for SP+KP-SPN increased from 192 nm to 241, 272 and 304 nm and at the end of 1, 2 and 3 months, respectively at accelerated storage conditions signifying

that the particle size was increased with an increase in storage temperature. Similarly the SP-SPN or KP-SPN showed a significant increase in particle size when stored at 40°C/75% RH.

3.6 *In vitro* skin permeation

SP was found below the detectable limit in receiver compartment after 24 h of human skin permeation using SP gel and SP-SPN or SP+KP-SPN. These results are comparable with previous reports from our laboratory, where SP was not detected in the receiver compartment upon application of SP lotion and gel on the rat skin [35]. SC, epidermal and dermal retention of SP for SP-SPN was 7.34, 5.32 and 1.14 mg/g of skin, respectively (Figure 3a). SP retained in SC, epidermis and dermis after application of SP-SPN was significantly different ($p < 0.001$) than the SP gel. Further the amount of SP retained in epidermis and dermis after application of SP-SPN or SP+KP-SPN was 1.5 and 2.7 times higher, respectively, than SP-NPSO or SP+KP-NPSO. KP was detectable in receiver compartment and 21.58 and 30.21 $\mu\text{g}/\text{cm}^2$ was permeated through the skin in case of KP-NPSO and KP-SPN, respectively (Figure 3c). The amount of KP in receiver compartment for KP-SPN was increased by 1.3 times than KP-NPSO. The skin retention of KP-SPN in various skin layers like SC, epidermal and dermal retention was 0.78, 0.41 and 0.23 mg/g of skin, respectively (Figure 3b). Further KP retained in SC, epidermis and dermis after KP-SPN application was significantly different ($p < 0.001$) than the KP-gel. The amount of KP retained in epidermis and dermis after application of KP-SPN or SP+KP-SPN was 1.4 and 2.1 times higher, respectively, than KP-NPSO or SP+KP-NPSO. Further the amount of KP or SP retained in various skin layers was not statistically different for SPN comprising individual drugs (KP-SPN or SP-SPN) and a combination of KP and SP, signifying lack of any interaction of SP on skin permeation of KP or vice versa.

3.7 *In vivo* inflammatory model

3.7.1 Allergic contact dermatitis (ACD)—The reduction of ear swelling of the inflamed mice ears was used to monitor the treatment of inflammation after application of SPN. The effect of gel and SPN on reduction of ear swelling is shown in Figure 4. The ear thickness was increased from 128.34 to 148.46 μm with time for control animals from 0 to 72 h. However after topical application of KP-gel and SP+KP-SPN for 3 consecutive days, the ear thickness was decreased to 106.56 and 56.23 μm , respectively. Similarly for SP-gel and SP+KP-SPN, it was decreased to 115.78 and 61.89 μm , respectively. There was no statistical difference in ear thickness before and after application of Topgraf[®]. The ear thickness for SP+KP-gel and SP+KP-SPN was 68.42 and 12.44 μm , respectively. The combination index value calculated from the ACD response ranged from 0.72 to 0.77 over an entire study period (0 to 72 h).

3.7.2 Imiquimod (IMQ) induced psoriatic plaque like model—Induction of psoriatic like plaques was performed by topical application of IMQ for 5 consecutive days. The scaling of the mice back skin, a phenomenon typical for psoriatic skin lesions, was observed after topical application of IMQ (Figure 5a). Analysis of H&E-stained sections from the IMQ-treated skin showed increased epidermal thickening with elongation of epidermal rete ridges, a disturbed epidermal differentiation and infiltration of leukocytes into both, dermis and epidermis (Figure 5b). In addition, the expression of IL-17 and IL-23 was significantly less ($p < 0.001$) for SP+KP-SPN compared to control IMQ treated mice (Figure 6). The PASI score for control was 4 at the end of 5th day (Table 2). However the PASI score for SP+KP-gel and SP+KP-SPN was decreased to 3 and 1, respectively at the end of 5th day. For Topgraf[®], PASI score was zero at the end of 2nd day of treatment. Similarly the TEWL values for SPN and Topgraf[®] were significantly less than control and gel (Figure 7). The combination index value calculated from TEWL value ranged from 0.69 to 0.74 over the entire period of the study (0 to 5 days).

4. Discussion

Allergic contact dermatitis (ACD) and psoriasis are the most common inflammatory skin disorders. It is desired that the anti-inflammatory drug should be delivered to the deeper skin layers where inflammation occurs. Nanoparticles have shown promising results in enhancing the drug delivery to the deep epidermis. Preliminary experiments in our laboratory have demonstrated that ibuprofen can be delivered in higher amounts to the deeper skin layers when applied in the form of PLGA and chitosan bilayered nanoparticles, modified with oleic acid (OA) (unpublished data). In the present study, we have incorporated these surface modified nanoparticles containing SP and KP into a gel formulation (SPN) to further enhance the drug delivery to the deeper skin layers by improving the contact time and avoiding water loss from the skin.

To prepare a SPN system, HPMC and Carbopol were selected as gelling agents. HPMC was selected as a gelling agent because it formed a homogenous dispersion due to its high water solubility whereas carbopol formed gel after addition of alkaline reagent, resulting in an increase in particle size of SPN. The effect of different percent of HPMC on viscosity profile and particle size of SPN was investigated since minimum particle size was desired along with the viscous gel. With 1.2% w/v HPMC, the viscosity and particle size was increased due to cross-linking of the polymer network. Similar observations have been reported for hydroxyl propyl cellulose (HPC) and HPMC gels becoming increasingly viscous due to increase in HPC and HPMC concentration [34]. Therefore lower percent of HPMC (0.8% w/v) was used for preparation of a SPN which did not show any change in the particle size. The SPN prepared using 0.8% w/v HPMC was further investigated for the rheological behavior since the spreadability of the topical formulation and contact time on the skin surface is directly related to the rheological behavior of the gel [32–34]. When the shear rate of SPN comprising 0.8% w/v was increased (up curve), shear stress was also increased with yield value, indicating pseudoplastic (non-Newtonian) behavior. Further, when the shear stress of NPS was decreased from 110 to 20 Pa (down curve), shear stress was also decreased proportionately, demonstrating thixotropic (shear-thinning) properties, which is desirable for topical formulations [36]. Therefore, based on viscosity, rheological properties and particle size, 0.8% w/v HPMC was selected for further investigation of drug release, stability, skin permeation studies and therapeutic efficacy in animal models.

The drug release from KP-SPN followed Korsmeyer–Peppas kinetics demonstrating that the drug was released in a controlled manner by a combination of both diffusion and erosion mechanisms. However, the drug release from SP-SPN followed first order kinetics which suggested that the drug release was dependent on the drug concentration. The controlled drug release from SPN might be because of an increase in viscosity of SPN associated with increase in percent of HPMC and a longer diffusion pathway [37]. Further, the SPN stored at refrigeration temperature showed excellent stability without significantly affecting particle size during the study period, which might be because of the hydration effect of HPMC. However, a gradual increase in particle size and PI values was observed at accelerated storage conditions signifying that the particle size was increased with an increase in storage temperature. Similar results were reported during the stability study of tacrolimus loaded lipid nanoparticle gel where a gradual increase in particle size and PI values was observed when stored at 30°C/65% RH and 40°C/75% RH for 3, 6 and 12 months. However, the gel stored at refrigeration condition remained stable with almost no change in particle size without any significant increase in PI values during the study period of 12 months [38].

Skin permeation studies showed a significant increase in SP and KP retention in deeper skin along with increase in the amount of KP permeated in receiver compartment for the SPN compared to NPSO and control gel formulations containing SP and KP. These results are

comparable to the reports with hydrogel containing KP-lipid nanoparticles which showed approximately 2.4 folds improvement in skin permeation compared to control KP-gel formulation [39]. Similar results were reported for gel comprising polymeric nanospheres and lipid nanoparticles [38]. The gel enriched with nile red containing polymeric nanospheres showed 1.4 folds increase in skin permeation of nile red than aqueous polymeric nanospheres [23]. In addition, Pople and Singh demonstrated that the permeation rate of tacrolimus from a gel containing tacrolimus lipid nanoparticles was almost 16–21 times higher than marketed tacrolimus ointment, Protopic[®]. This might be because of the increase in drug release from gel containing tacrolimus lipid nanoparticles than protopic ointment [38]. Furthermore the amount of KP or SP retained in various skin layers was not statistically different for SPN comprising individual drugs (KP or SP) and a combination of KP and SP, signifying lack of interaction of SP on skin permeation of KP.

During the inflammatory skin disorders like ACD and psoriasis, various cytokines, chemokines, eicosanoids [40] and substance P [41] are reported to be involved in the regulation of inflammatory process. ACD, an acute inflammation, is characterized by classical symptoms such as heat, redness, swelling and pain [42]. DNFB induced edema (after secondary exposure) is widely used for investigating cutaneous inflammatory process [35]. Further, IMQ has been reported to induce skin inflammation in mice along with the features of human psoriasis where cytokines like IL-23 and IL-17 levels are elevated with typical phenotypic and histological characteristics [28, 43–45]. Therefore the efficacy of SPNs was investigated in two inflammatory models with different end points. SP is known to antagonize substance P by competitively binding to neurokinin-1 receptors present on the cutaneous cells for inhibition of capsaicin-induced [46] and DNFB-induced [35] ear edema in mice. Further KP has been reported to inhibit prostaglandin (PG) biosynthesis and maturation of Langerhans cells to show anti-inflammatory effect [47]. The results of ACD model demonstrate that SPNs containing a combination of SP and KP improved effectiveness in reducing acute cutaneous inflammation. To evaluate the additive or synergistic effect, the combination index value was calculated based on the response of ACD model. The combination index value calculated for each day suggested moderate synergism for SP+KP-SPN over the entire study period which might be because of two different mechanisms of SP and KP working together in reducing the cutaneous inflammation associated with ACD. These results were further confirmed by the psoriatic plaque like model where the epidermal thickening, elongation of epidermal rete ridges, infiltration of leukocytes, IL-23 and IL-17 levels were significantly less ($p < 0.001$) in SP +KP-SPN compared to SP+KP-gel and control, signifying the effectiveness of the SP+KP-SPN. Furthermore, the TEWL values of psoriatic plaque like model were significantly lower ($p < 0.001$) for SP+KP-SPN than control mice further confirming the moderate synergistic behavior of the two drugs. However Topgraf[®], a commercial tacrolimus formulation was slightly more effective ($p < 0.05$) than the SP+KP-SPN which was expected since tacrolimus is a new and powerful macrolide immunosuppressant and has shown notable efficacy against inflammatory conditions like ACD and psoriasis. Being a calcineurin inhibitor, it significantly reduces the number of various epidermal and dermal T-cell subsets [48]. However, the thrust of this research is to demonstrate that our SPN containing surface modified nanoparticles can deliver two anti-inflammatory agents having varied mechanisms to the deeper skin layers with possible synergistic activity.

Future studies will be directed to use of more potent drugs with the SPN formulations for the treatment of various skin disorders like allergic contact dermatitis and psoriasis.

Conclusion

Our studies demonstrate that the nanogel comprising surface modified nanoparticles (NPSO) enhanced skin permeation of spantide II and ketoprofen by translocating the nanoparticles across the deeper skin layers by improving skin contact time and hydration of the skin by forming a thin layer on the skin surface (occlusive effect). Thus, the increase in skin permeation of spantide II and ketoprofen was further responsible for improved response in ACD and psoriatic plaque like model suggesting the potential of the combination therapy to treat various inflammatory skin disorders like ACD and psoriasis. In addition, there was no interaction between the spantide II and ketoprofen during *in vitro* skin permeation and drug release studies. Similar approach could be extrapolated to treat other skin diseases like fungal, bacterial, viral- infections and skin cancers like melanoma.

Acknowledgments

We thank Ms. Debra Channer for her technical help. The authors acknowledge the financial assistance provided by RCMI (NIH) grant number G12RR03020.

References

1. Wang ZH, Wang ZY, Sun CS, Wang CY, Jiang TY, Wang SL. Trimethylated chitosan-conjugated PLGA nanoparticles for the delivery of drugs to the brain. *Biomaterials*. 2010; 31:908–15. [PubMed: 19853292]
2. Sultana Y, Maurya DP, Iqbal Z, Aqil M. Nanotechnology in ocular delivery: current and future directions. *Drugs Today (Barc)*. 2011; 47:441–55. [PubMed: 21695286]
3. Patlolla RR, Chougule M, Patel AR, Jackson T, Tata PN, Singh M. Formulation, characterization and pulmonary deposition of nebulized celecoxib encapsulated nanostructured lipid carriers. *J Control Release*. 2010; 144:233–41. [PubMed: 20153385]
4. Pan Y, Li YJ, Zhao HY, Zheng JM, Xu H, Wei G, et al. Bioadhesive polysaccharide in protein delivery system: chitosan nanoparticles improve the intestinal absorption of insulin in vivo. *Int J Pharm*. 2002; 249:139–47. [PubMed: 12433442]
5. Slutter B, Bal S, Keijzer C, Mallants R, Hagens N, Que I, et al. Nasal vaccination with N-trimethyl chitosan and PLGA based nanoparticles: nanoparticle characteristics determine quality and strength of the antibody response in mice against the encapsulated antigen. *Vaccine*. 2010; 28:6282–91. [PubMed: 20638455]
6. Lee PW, Hsu SH, Tsai JS, Chen FR, Huang PJ, Ke CJ, et al. Multifunctional core-shell polymeric nanoparticles for transdermal DNA delivery and epidermal langerhans cells tracking. *Biomaterials*. 2010; 31:2425–34. [PubMed: 20034662]
7. Barry BW. Novel mechanisms and devices to enable successful transdermal drug delivery. *Eur J Pharm Sci*. 2001; 14:101–14. [PubMed: 11500256]
8. Jensen LB, Petersson K, Nielsen HM. In vitro penetration properties of solid lipid nanoparticles in intact and barrier-impaired skin. *Eur J Pharm Biopharm*. 2011; 79:68–75. [PubMed: 21664463]
9. Babu RJ, Kikwai L, Jaiani LT, Kanikkannan N, Armstrong CA, Ansel JC, et al. Percutaneous absorption and anti-inflammatory effect of a substance P receptor antagonist: spantide II. *Pharm Res*. 2004; 21:108–13. [PubMed: 14984264]
10. Kikwai L, Babu RJ, Kanikkannan N, Singh M. Preformulation stability of spantide II, a promising topical anti-inflammatory agent for the treatment of psoriasis and contact dermatitis. *J Pharm Pharmacol*. 2004; 56:19–25. [PubMed: 14979997]
11. Shinkai N, Korenaga K, Okumura Y, Mizu H, Yamauchi H. Microdialysis assessment of percutaneous penetration of ketoprofen after transdermal administration to hairless rats and domestic pigs. *Eur J Pharm Biopharm*. 2011; 78:415–21. [PubMed: 21397690]
12. Rancan F, Papakostas D, Hadam S, Hackbarth S, Delair T, Primard C, et al. Investigation of polylactic acid (PLA) nanoparticles as drug delivery systems for local dermatotherapy. *Pharm Res*. 2009; 26:2027–36. [PubMed: 19533305]

13. Lademann J, Richter H, Teichmann A, Otberg N, Blume-Peytavi U, Luengo J, et al. Nanoparticles- an efficient carrier for drug delivery into the hair follicles. *Eur J Pharm Biopharm.* 2007; 66:159–64. [PubMed: 17169540]
14. Alvarez-Roman R, Barre G, Guy RH, Fessi H. Biodegradable polymer nanocapsules containing a sunscreen agent: preparation and photoprotection. *Eur J Pharm Biopharm.* 2001; 52:191–5. [PubMed: 11522485]
15. Colonna C, Conti B, Perugini P, Pavanetto F, Modena T, Dorati R, et al. Ex vivo evaluation of prolidase loaded chitosan nanoparticles for the enzyme replacement therapy. *Eur J Pharm Biopharm.* 2008; 70:58–65. [PubMed: 18547793]
16. Jain GK, Pathan SA, Akhter S, Ahmad N, Jain N, Talegaonkar S, et al. Mechanistic study of hydrolytic erosion and drug release behaviour of PLGA nanoparticles: influence of chitosan. *Polymer Degrad Stab.* 2010; 95:2360–6.
17. Senyigit T, Sonvico F, Barbieri S, Ozer O, Santi P, Colombo P. Lecithin/chitosan nanoparticles of clobetasol-17-propionate capable of accumulation in pig skin. *J Control Release.* 2010; 142:368–73. [PubMed: 19932722]
18. Alvarez-Roman R, Naik A, Kalia YN, Guy RH, Fessi H. Enhancement of topical delivery from biodegradable nanoparticles. *Pharm Res.* 2004; 21:1818–25. [PubMed: 15553228]
19. Luengo J, Weiss B, Schneider M, Ehlers A, Stracke F, Konig K, et al. Influence of nanoencapsulation on human skin transport of flufenamic acid. *Skin Pharmacol Physiol.* 2006; 19:190–7. [PubMed: 16679821]
20. Rowat AC, Kitson N, Thewalt JL. Interactions of oleic acid and model stratum corneum membranes as seen by 2H NMR. *Int J Pharm.* 2006; 307:225–31. [PubMed: 16293379]
21. Tanojo H, Bos-van Geest A, Bouwstra JA, Junginger HE, Boodé HE. In vitro human skin barrier perturbation by oleic acid: thermal analysis and freeze fracture electron microscopy studies. *Thermochimica Acta.* 1997; 293:77–85.
22. Samah NA, Williams N, Heard CM. Nanogel particulates located within diffusion cell receptor phases following topical application demonstrates uptake into and migration across skin. *Int J Pharm.* 2010; 401:72–8. [PubMed: 20817080]
23. Batheja P, Sheihet L, Kohn J, Singer AJ, Michniak-Kohn B. Topical drug delivery by a polymeric nanosphere gel: formulation optimization and in vitro and in vivo skin distribution studies. *J Control Release.* 2011; 149:159–67. [PubMed: 20950659]
24. Yuan X, Shah BA, Kotadia NK, Li J, Gu H, Wu Z. The development and mechanism studies of cationic chitosan-modified biodegradable PLGA nanoparticles for efficient siRNA drug delivery. *Pharm Res.* 2010; 27:1285–95. [PubMed: 20309616]
25. Patlolla RR, Desai PR, Belay K, Singh MS. Translocation of cell penetrating peptide engrafted nanoparticles across skin layers. *Biomaterials.* 2010; 31:5598–607. [PubMed: 20413152]
26. Kouchakzadeh H, Shojaosadati S, Maghsoudi A, Vasheghani Farahani E. Optimization of PEGylation conditions for BSA nanoparticles using response surface methodology. *AAPS Pharm Sci Tech.* 2010; 11:1206–11.
27. Ghouchi Eskandar N, Simovic S, Prestidge C. Nanoparticle coated submicron emulsions: sustained *in vitro* release and improved dermal delivery of all-trans-retinol. *Pharm Res.* 2009; 26:1764–75. [PubMed: 19384464]
28. van der Fits L, Mourits S, Voerman JS, Kant M, Boon L, Laman JD, et al. Imiquimod-induced psoriasis-like skin inflammation in mice is mediated via the IL-23/IL-17 axis. *J Immunol.* 2009; 182:5836–45. [PubMed: 19380832]
29. Chatterjee A, Babu R, Klausner M, Singh M. *In vitro* and *in vivo* comparison of dermal irritancy of jet fuel exposure using EpiDerm (EPI-200) cultured human skin and hairless rats. *Toxicol Lett.* 2005; 167:85–94. [PubMed: 17049765]
30. Chougule MB, Patel A, Jackson T, Singh M. Antitumor activity of noscapine in combination with doxorubicin in triple negative breast cancer. *PLoS One.* 2011; 6:e17733. [PubMed: 21423660]
31. Chougule MB, Patel AR, Sachdeva P, Jackson T, Singh M. Anticancer activity of noscapine, an opioid alkaloid in combination with cisplatin in human non-small cell lung cancer. *Lung Cancer.* 2011; 71:271–82. [PubMed: 20674069]

32. Lee CH, Moturi V, Lee Y. Thixotropic property in pharmaceutical formulations. *J Control Release*. 2009; 136:88–98. [PubMed: 19250955]
33. Mortazavi SA, Tabandeh H. The influence of various silicones on the rheological parameters of AZG containing silicone-based gels. *Iran J Pharm Res*. 2005; 4:205–11.
34. Ramachandran S, Chen S, Etzler F. Rheological characterization of hydroxypropylcellulose gels. *Drug Dev Ind Pharm*. 1999; 25:153–61. [PubMed: 10065348]
35. Kikwai L, Babu RJ, Prado R, Kolot A, Armstrong CA, Ansel JC, et al. In vitro and in vivo evaluation of topical formulations of spantide II. *AAPS Pharm Sci Tech*. 2005; 6:E565–72.
36. Pena LE, Lee BL, Stearns JF. Structural rheology of a model ointment. *Pharm Res*. 1994; 11:875–81. [PubMed: 7937529]
37. Baumgartner S, Kristl J, Peppas NA. Network structure of cellulose ethers used in pharmaceutical applications during swelling and at equilibrium. *Pharm Res*. 2002; 19:1084–90. [PubMed: 12240932]
38. Pople P, Singh KK. Targeting tacrolimus to deeper layers of skin with improved safety for treatment of atopic dermatitis. *Int J Pharm*. 2010; 398:165–78. [PubMed: 20637847]
39. Puglia C, Blasi P, Rizza L, Schoubben A, Bonina F, Rossi C, et al. Lipid nanoparticles for prolonged topical delivery: an *in vitro* and *in vivo* investigation. *Int J Pharm*. 2008; 357:295–304. [PubMed: 18343059]
40. Choi SP, Kim SP, Kang MY, Nam SH, Friedman M. Protective effects of black rice bran against chemically-induced inflammation of mouse skin. *J Agric Food Chem*. 2010; 58:10007–15. [PubMed: 20731354]
41. Ansel JC, Kaynard AH, Armstrong CA, Olerud J, Bunnett N, Payan D. Skin-nervous system interactions. *J Invest Dermatol*. 1996; 106:198–204. [PubMed: 8592075]
42. Cabrini, DA.; Moresco, H.; Imazu, P.; da Silva, CD.; Pietrovski, EF.; Mendes, DA., et al. Analysis of the potential topical anti-inflammatory activity of *averrhoa carambola* L. in mice. *Evid Based Complement Alternat Med*. 2011. Available from URL: <http://www.hindawi.com/journals/ecam/2011/908059/>
43. Tsuruta D. NF-kappa-B links keratinocytes and lymphocytes in the pathogenesis of psoriasis. *Recent Pat Inflamm Allergy Drug Discov*. 2009; 3:40–8. [PubMed: 19149745]
44. Guilloteau K, Paris I, Pedretti N, Boniface K, Juchaux F, Huguier V, et al. Skin inflammation induced by the synergistic action of IL-17A, IL-22, oncostatin M, IL-1{alpha}, and TNF-{\alpha} recapitulates some features of psoriasis. *J Immunol*. 2010; 184:5263–70.
45. Fujisawa H, Shivji G, Kondo S, Wang B, Tomai MA, Miller RL, et al. Effect of a novel topical immunomodulator, S-28463, on keratinocyte cytokine gene expression and production. *J Interferon Cytokine Res*. 1996; 16:555–9. [PubMed: 8836922]
46. Inoue H, Nagata N, Koshihara Y. Involvement of substance P as a mediator in capsaicin-induced mouse ear oedema. *Inflamm Res*. 1995; 44:470–4. [PubMed: 8597880]
47. Atarashi K, Kabashima K, Akiyama K, Tokura Y. Skin application of the nonsteroidal anti-inflammatory drug ketoprofen downmodulates the antigen-presenting ability of langerhans cells in mice. *Br J Dermatol*. 2008; 159:306–13. [PubMed: 18565185]
48. Vissers WH, van Vlijmen I, van Erp PE, de Jong EM, van de Kerkhof PC. Topical treatment of mild to moderate plaque psoriasis with 0.3% tacrolimus gel and 0.5% tacrolimus cream: the effect on SUM score, epidermal proliferation, keratinization, T-cell subsets and HLA-DR expression. *Br J Dermatol*. 2008; 158:705–12. [PubMed: 18284400]

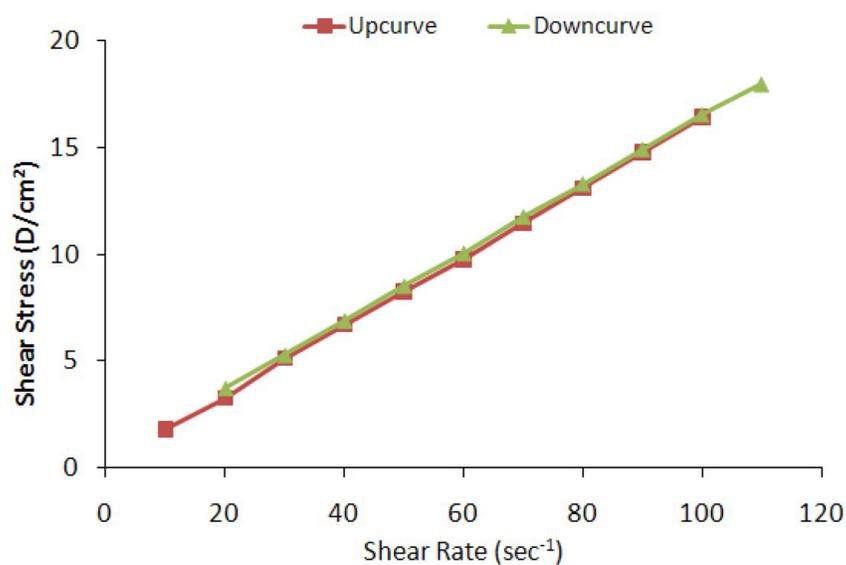


Figure 1. Rheology of skin penetrating nanogel (SPN) showing correlation between shear stress and shear rate. When the shear rate of nanogel was increased (up curve), shear stress was also increased with yield value, indicating pseudoplastic (non-Newtonian) behavior. Further when the shear stress of nanogel was decreased from 110 to 20 (down curve), shear stress was also decreased proportionately, demonstrating thixotropic (shear-thinning) properties of the SPNs.

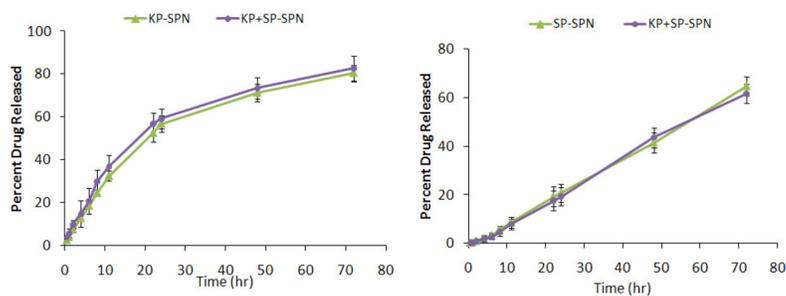


Figure 2.

In vitro drug release of a) spantide II (SP) and b) ketoprofen (KP) from KP and SP comprising skin penetrating nanogels (SPNs) in PBS (pH 7.4) containing 0.5% w/v volpo. The cumulative amount released was plotted against time. The drug release studies with SP-SPN or KP-SPN and SP+KP-SPN showed no significant difference between the KP and SP release when used alone or in combination, signifying no interaction between the drug release of SP and KP. Data represent mean \pm SEM, n=6.

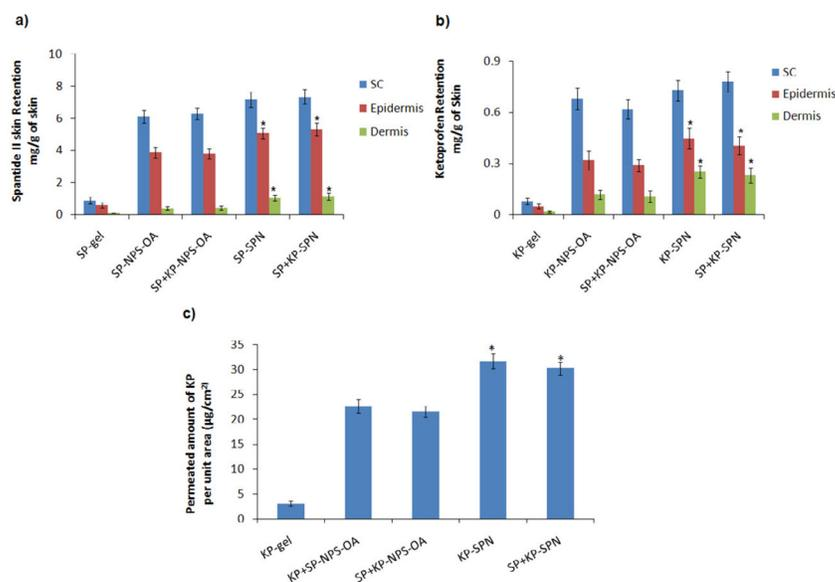


Figure 3. Effect of control gel, aqueous dispersion of surface modified bilayered nanoparticles (NPSO) and skin penetrating nanogels (SPNs) on the skin retention of a) spantide II (SP) and b) ketoprofen (KP). *In vitro* skin permeation studies were performed in dermatomed human skin using Franz diffusion cells and after 24 h of application, the skin was collected and processed as described in methods section. The amount of SP and KP retained in epidermis and dermis after application of SPNs is significantly higher than control gel. c) The amount of KP Permeated per unit area after 24 hrs of dermatomed human skin permeation study performed using control gel, aqueous NPSO and SPNs. Data represent mean \pm SD, n = 6, significance control gel against SPNs where * $p < 0.001$.

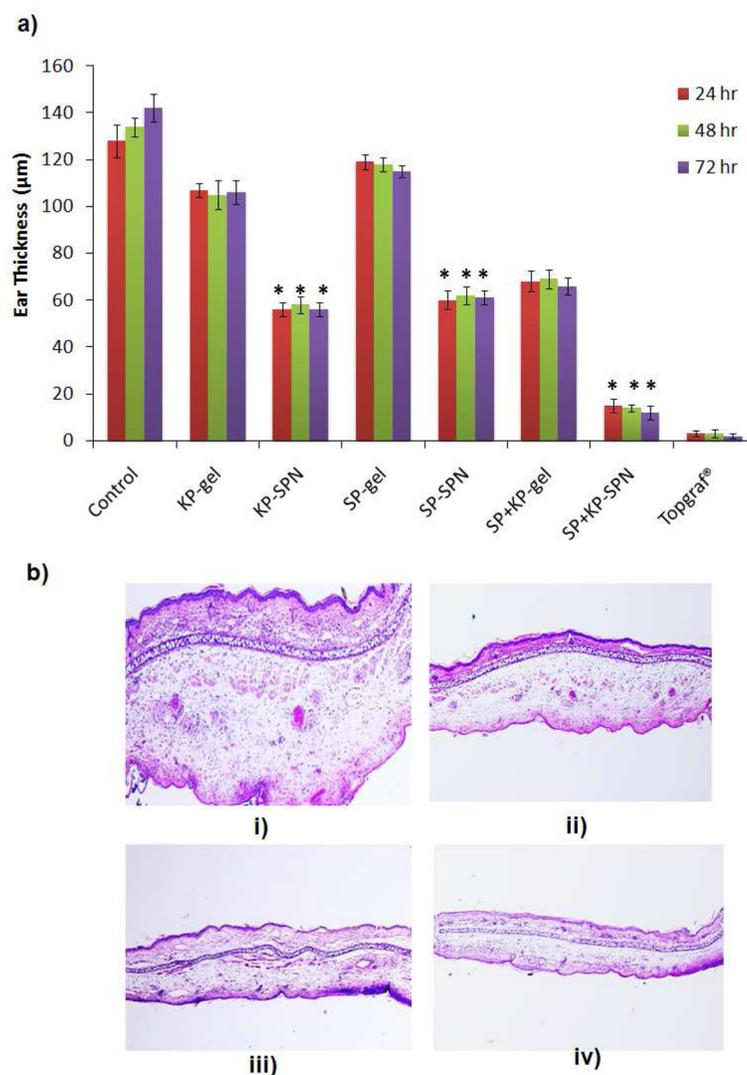


Figure 4.

a) Effect of control gel and skin penetrating nanogels (SPNs) containing SP and KP treatment on the response of allergic contact dermatitis (ACD) model in C57/BL mice. Data represent mean \pm SD, $n = 6$, significance gel against SPNs where $*p < 0.001$. b) H&E histological staining of i) inflammation induced by topical application of DNFB, and after 3 days treatment of ii) spantide II and ketoprofen comprising gel (SP+KP gel) iii) spantide II and ketoprofen comprising skin penetrating nanogels (SP+KP-SPN) and iv) a positive control, Topgraf® (tacrolimus ointment 0.1%).

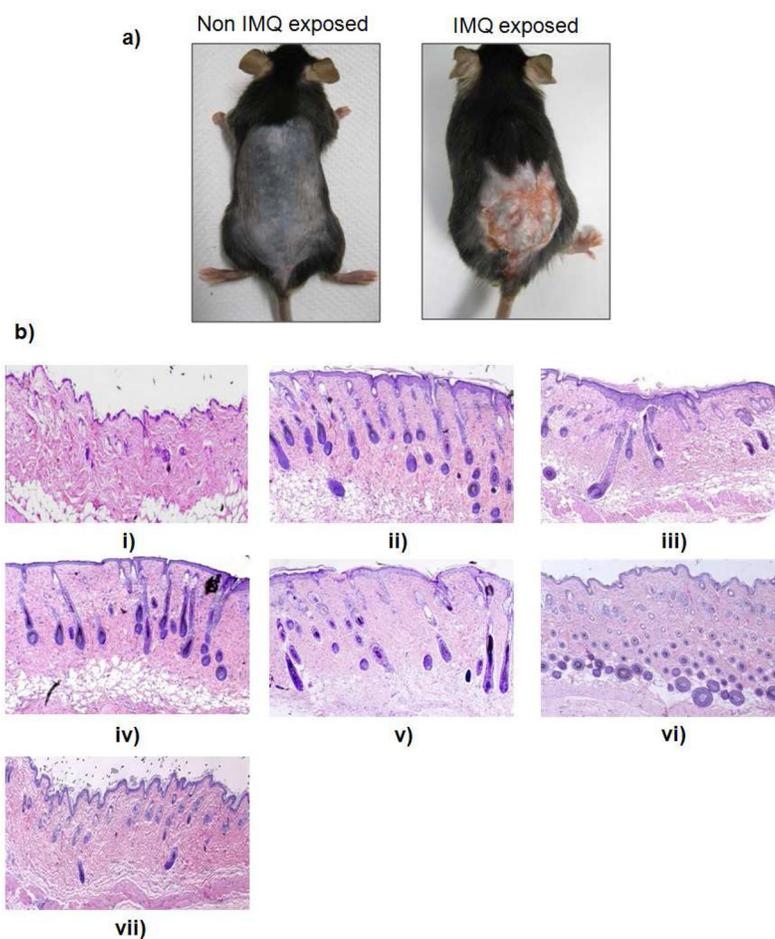


Figure 5.

a) IMQ exposure alters keratinocyte proliferation and differentiation. Mice were exposed to the IMQ suspension for 5 days. b) H&E histological staining of i) normal skin, ii) inflammation induced by topical application of IMQ suspension, and inflamed skin after 5 days treatment of iii) spantide II and ketoprofen comprising gel (SP+KP gel) iv) ketoprofen comprising skin penetrating nanogels (KPSPN) v) spantide II comprising skin penetrating nanogels (SP-SPN) vi) spantide II and ketoprofen comprising skin penetrating nanogels (SP+KP-SPN) and vii) a positive control, Topgraf[®] (tacrolimus ointment 0.1%).

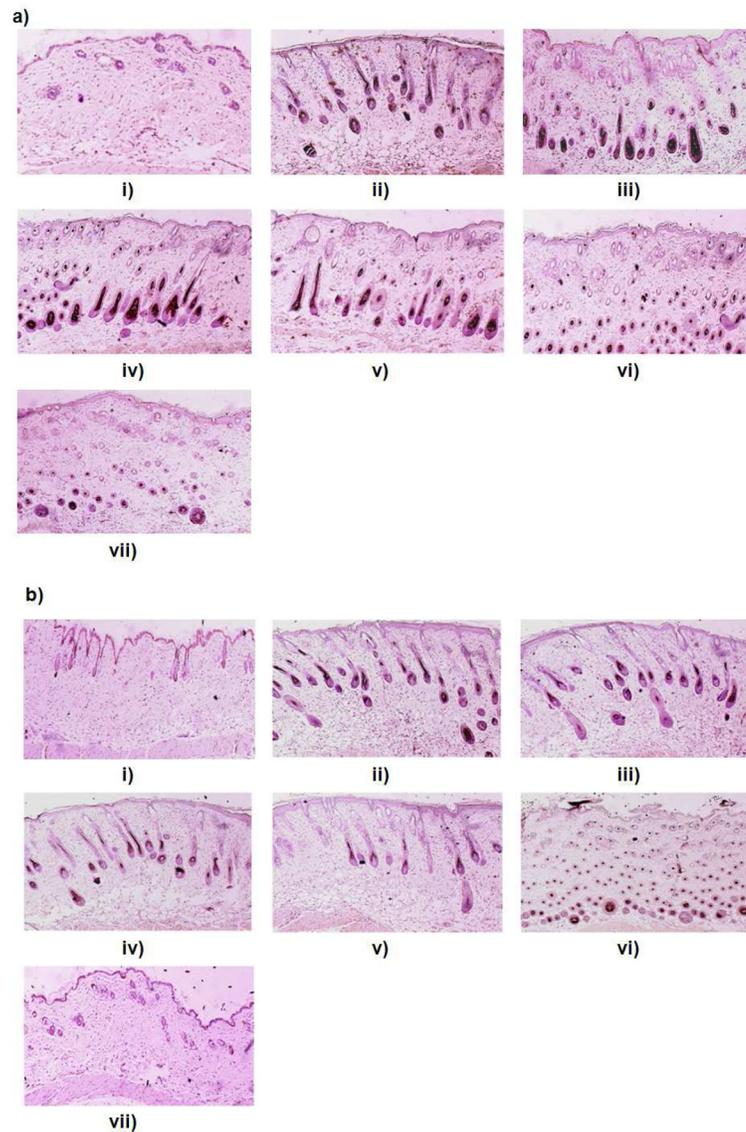


Figure 6. Immunohistochemistry a) IL-17 and b) IL-23 for i) normal skin, ii) inflamed skin induced by topical application of IMQ suspension, and inflamed skin after 5 days treatment of iii) spantide II and ketoprofen comprising gel (SP+KP gel) iv) ketoprofen comprising skin penetrating nanogels (KP-SPN) v) spantide II comprising skin penetrating nanogels (SP-SPN) vi) spantide II and ketoprofen comprising skin penetrating nanogels (SP+KP-SPN) and vii) a positive control, Topgraf[®] (tacrolimus ointment 0.1%). The presence of brown staining was considered a positive identification for activated IL-17 and IL-23.

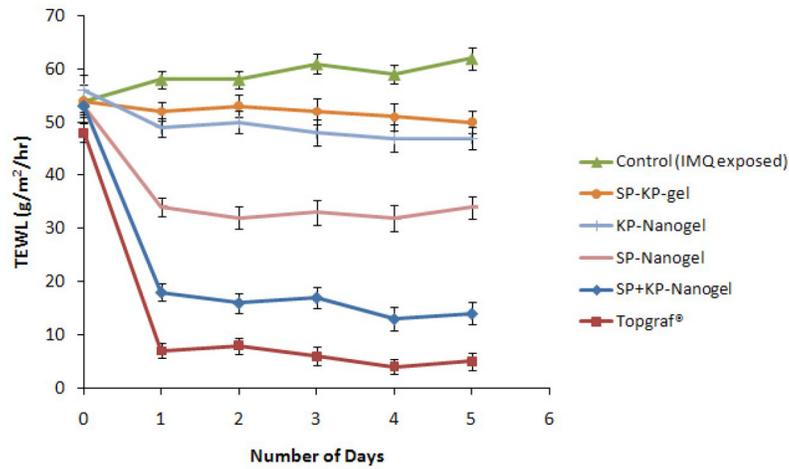


Figure 7.

Trans-epidermal water loss (TEWL) values of each day after treatment of spantide II and ketoprofen comprising gel (SP+KP gel) and skin penetrating nanogel comprising ketoprofen (KP-SPN), spantide II (SP-SPN), a combination of spantide II and ketoprofen (SP+KP-SPN) along with a positive control, Topgraf® (tacrolimus ointment 0.1%) for 5 days on the back skin of C57/BL mice. Values represent mean \pm SD, n = 6.

Table 1

Effect of percent of HPMC on viscosity and particle size of SPNs

HPMC w/v	Viscosity (cP), 25 °C ± SD	Particle Size (nm) ± SD
0.4%	0.12 ± 0.02	187 ± 14
0.8%	1.16 ± 0.03	192 ± 11
1.2%	13.43 ± 0.02	226 ± 16

Table 2

IMQ-induced skin inflammation in mice phenotypically resembles psoriasis. C57BL/6 mice were treated daily for 5 days with IMQ suspension on the shaved back skin and then the inflamed area was treated with SP+KP gel, SPNs and Topgraf[®]. Psoriasis Area and Severity Index (PASI) score of the back skin was recorded daily on a scale from 0 to 4.

Day	Control (No treatment)	SP+KP-gel	KP-SPN	SP-SPN	SP+KP-SPN	Topgraf [®]
0	4	4	4	4	4	4
1	4	4	4	4	3	1
2	4	4	4	3	3	0
3	4	4	3	3	2	0
4	4	3	3	2	2	0
5	4	3	3	2	1	0